

Multimodal Sensor Fusion for Attitude Control of Micromechanical Flying Insects: a Geometric Approach

Domenico Campolo, Luca Schenato, and Eugenio Guglielmelli

(Regular Paper)

Abstract— In this paper, we study sensor fusion for the attitude stabilization of Micro Aerial Vehicles (MAVs), in particular mechanical flying insects. First, following a geometric approach, a dynamic observer is proposed which estimates attitude based on kinematic data available from different and redundant bio-inspired sensors such as halteres, ocelli, gravitometers, magnetic compass and light polarization compass. In particular, the traditional structure of complementary filters, suitable for multiple sensor fusion, is specialized to the Lie group of rigid body rotations $SO(3)$ by means of an intrinsic notion of state error. A natural Lyapunov function is then defined to prove almost-global asymptotic stability of the proposed observer. Second, stability of traditional passivity-based attitude controllers is proved also in the case when the output of the proposed dynamic observer is used as state feedback. Finally, simulations are used to demonstrate greater robustness to disturbances of dynamic attitude estimation feedback as compared with static output feedback.

keywords: sensor fusion, ocelli, halteres, gravitometer, polarization sensor, attitude control, $SO(3)$ Lie group

I. INTRODUCTION

Today there are several successful examples of autonomous flying vehicles, from airplanes [18] to helicopters [19]. However, their size hamper their use in surveillance and search-and-rescue missions in urban areas, in indoor environments and in natural disaster scenarios as after earthquakes. Therefore, there is an increasing need for very small size air vehicles with high performance. In particular, the current trend is to study micro aerial vehicles (MAVs) using traditional air-vehicle paradigms such as fixed-winged air-vehicles [16] or rotorcrafts [20]. Differently, inspired by the unmatched maneuverability and hovering capability by real insects, some groups have started using biomimetic principles to develop micromechanical flying insects (MFIs) with flapping wings that will be capable of sustained autonomous flight [14], [25].

The extraordinary performance of flying insects is the result of two peculiar features: the first feature is the enhanced *unsteady-state aerodynamic* forces and moments generated by the flapping wings [29], [34], [11], and the second feature is the *multimodal sensor fusion*, i.e. the ability to integrate

information from a number of different and redundant sensors to reduce the effect of noise and external disturbances [37], [13].

In this paper, we focus explicitly on the latter feature of insect flight, i.e. on sensor fusion of redundant information for attitude control, and we assume that we can control directly the torque applied to the insect body as shown in [11]. Although sensor fusion and filtering have been studied for decades and many results are available for linear spaces [2], it remains a hard problem on the Lie group of rigid body rotations $SO(3)$ where standard tools like Kalman filtering cannot be applied directly. Theory of complementary and Kalman filters has traditionally been used to design attitude observers, especially in presence of redundant measurements. Kalman filters were originally developed for linear systems and then extended to cope with nonlinearities via linearization techniques. On the other hand, complementary filters are capable of fully exploiting the rich nonlinear structure underlying problems such as rigid body rotations, well described by the theory of Lie groups.

As a first contribution of this work, the traditional structure of complementary filters is specialized to the Lie group of rigid body rotations $SO(3)$. In particular, a dynamic observer is proposed which derives an attitude estimate from redundant information typically available from bio-inspired sensors. Following the geometric approach of [21], [4], [24], this is achieved by avoiding the parametrization step. The proposed observer is based on a notion of state error which is *intrinsic*, so its performance does not depend on an arbitrary choice of coordinates, and *coordinate-free*, in the sense that the equations may be written explicitly without specifying coordinates for the configuration space. Stability of the observer is proved via a “natural” Lyapunov function.

The second contribution of this work is related to the attitude stabilization of mechanical flying insects once a state estimate is available from bio-inspired sensors via a dynamic observer. In fact, traditionally, attitude stabilization via state feedback is achieved via passivity-based control [32] but stability concerns arise when the state is estimated by a dynamic observer, since this would introduce extra dynamics. To this end, the “separation principle” from [23] is used to prove that the proposed complementary filter and a traditional passivity-based attitude control system can be coupled to stabilize attitude of a mechanical flying insect.

Section II briefly reviews necessary notation, definitions and

Corresponding author: d.campolo@unicampus.it

Domenico Campolo and Eugenio Guglielmelli are with the Biomedical Robotics & EMC Laboratory of the Università Campus Bio-Medico, 00155 Roma - Italy.

Luca Schenato is with the Department of Information Engineering of the University of Padova, 35131 Padova - Italy.

metric properties concerning the Lie group $SO(3)$ of rigid body rotations. Section III reviews flying insect dynamics and the navigation sensory system of real insects. In Section IV, a complementary filter approach is proposed for sensor fusion. In Section V the dynamic output from the proposed observer is used as a feedback for traditional state-feedback attitude controller. In Section VI simulations are used to show the benefits of dynamic attitude estimation with respect to non-dynamic one in presence of disturbances.

II. MATHEMATICAL BACKGROUND

This section briefly describes the notation and several geometric notions that will be used throughout the paper. For additional details, the reader is referred to texts such as [1], [15], [26], [31], [3].

A. Basic Definitions

As shown in [1], [26], the natural configuration space for a rigid body is the *Lie group* $SO(3)$, i.e. the configuration of a rigid body can always be represented by a rotation matrix R , i.e. a matrix such that $R^{-1} = R^T$ and $\det R = +1$. Consider now the coordinate frames \mathbb{R}_S^3 and \mathbb{R}_B^3 :

- $\mathbb{R}_S^3 \approx \mathbb{R}^3$: the *space* coordinate frame, or initial configuration frame.
- $\mathbb{R}_B^3 \approx \mathbb{R}^3$: the *body* frame, which is attached to the body (can be thought of as defined by the sensors sensitive axis), initially coincident with the space frame.

An element R of $SO(3)$ can be thought of as a map from the body frame to the space frame, i.e. $R : \mathbb{R}_B^3 \rightarrow \mathbb{R}_S^3$.

A trajectory of the rigid body is curve $R(t) : \mathbb{R} \rightarrow SO(3)$. The velocity vector \dot{R} is tangent to the group $SO(3)$ in R but, as shown in [1], [26], rather than considering \dot{R} , two important quantities are worth to be considered:

- $\dot{R}R^T$: representing the rigid body angular velocity relative to the space frame;
- $R^T\dot{R}$: representing the rigid body angular velocity relative to the body frame.

These are both elements of the *Lie algebra* $so(3)$, i.e. the tangent space to the group $SO(3)$ at the identity I .

Elements of the Lie algebra are represented by skew-symmetric matrices. Systems on Lie groups described in terms of body (space) coordinates are called *left-invariant (right-invariant)*.

Left-invariance: let $R_1(t)$ be a trajectory of a rigid body relative to a space frame $\mathbb{R}_{S_1}^3$. Consider a change of space frame $G : \mathbb{R}_{S_1}^3 \rightarrow \mathbb{R}_{S_2}^3$, now $R_2(t) = GR_1(t)$ represents the *same* trajectory but with respect to the new space frame. It is straightforward to verify that $R_2^T\dot{R}_2 = R_1^T\dot{R}_1$, i.e. the angular velocity relative to the body frame $R^T\dot{R}$ does not depend on the choice of space frame.

Right-invariance: similarly, it can be shown that the angular velocity of a rigid body relative to a space frame $\dot{R}R^T$ does not depend on the choice of coordinate frame attached to the body.

In the case of $SO(3)$, there exists [26] an isomorphism of vector spaces $\hat{\cdot} : so(3) \rightarrow \mathbb{R}^3$, referred to as *hat* operator,

that allows writing $so(3) \approx \mathbb{R}^3$. For a given vector $a = [a_1 \ a_2 \ a_3]^T \in \mathbb{R}^3$, we write:

$$\hat{\cdot} : a = \begin{bmatrix} a_1 \\ a_2 \\ a_3 \end{bmatrix} \longrightarrow \begin{bmatrix} 0 & -a_3 & a_2 \\ a_3 & 0 & -a_1 \\ -a_2 & a_1 & 0 \end{bmatrix} = \hat{a} \quad (1)$$

Denote $(\cdot)^\vee : \mathbb{R}^3 \rightarrow so(3)$ its inverse, referred to as *vee* operator:

$$(\cdot)^\vee : \hat{a} = \begin{bmatrix} 0 & -a_3 & a_2 \\ a_3 & 0 & -a_1 \\ -a_2 & a_1 & 0 \end{bmatrix} \longrightarrow \begin{bmatrix} a_1 \\ a_2 \\ a_3 \end{bmatrix} = (\hat{a})^\vee \quad (2)$$

The Lie algebra is equipped with an operator, the *Lie brackets* $[\cdot, \cdot]$ which is defined by the matrix commutator:

$$[\hat{a}, \hat{c}] = \hat{a}\hat{c} - \hat{c}\hat{a} = \widehat{a \times c} \quad (3)$$

where $a, c \in \mathbb{R}^3$, $\hat{a}, \hat{c} \in so(3)$ and \times is cross product in \mathbb{R}^3 .

Given a finite-dimensional vector space V , let V^* be its *dual* space, i.e. the space whose elements (*covectors*) are linear functions from V to \mathbb{R} . If $\sigma \in V^*$, then $\sigma : V \rightarrow \mathbb{R}$. Denote the value of σ on $v \in V$ by $\langle \sigma, v \rangle$, i.e. the *pairing* operator $\langle \cdot, \cdot \rangle : V^* \times V \rightarrow \mathbb{R}$.

If $V = \mathbb{R}^n$ then $V^* \simeq \mathbb{R}^n$. For all $v \in V$ and $\sigma \in V^* \simeq \mathbb{R}^n$ then

$$\begin{aligned} \langle \sigma, v \rangle &= \sigma^T a \\ \langle \hat{\sigma}, \hat{v} \rangle &= \frac{1}{2} \text{trace}(\hat{\sigma}^T \hat{v}) \end{aligned} \quad (4)$$

B. Metric properties of $SO(3)$

In what follows necessary background and geometric tools are reviewed in order to define a norm (a distance) on $SO(3)$. This will be used later to prove convergence of the proposed feedback.

On a general manifold M , a positive definite quadratic form $\langle \langle \xi_1, \xi_2 \rangle \rangle_{T_x M}$ defined on any tangent space $T_x M \ni \xi_1, \xi_2$ (the space tangent to M in $x \in M$) is called a *Riemannian metric* [1]. It is the equivalent of the scalar product in \mathbb{R}^n , can be used to measure the distance between different points of a manifold, in mechanics a metric is tightly linked to the definition of kinetic energy [3]. A metric is extra structure, does not come with the manifold. Many different metrics, i.e. many different distance measures, can be defined on the same manifold [1].

Lie groups are, by definition, manifolds and therefore are entitled to possess metric properties. Lie groups, in particular $SO(3)$, are structured in such a way that some metrics *naturally*¹ arise. A *left-invariant* metrics does not depend on the choice of the space frame, i.e. it only needs to be defined on the Lie algebra and then it can be left-translated to the tangent space at any other group element:

$$\langle \langle R\hat{a}, R\hat{c} \rangle \rangle_{T_{RSO(3)}} = \langle \langle \hat{a}, \hat{c} \rangle \rangle_{so(3)}$$

where $R \in SO(3)$ and $\hat{a}, \hat{c} \in so(3)$.

Still, there many choices for a metric in the Lie algebra, as many as there are positive definite matrices P :

$$\langle \langle \hat{a}, \hat{c} \rangle \rangle_{so(3)} \triangleq a^T P c$$

¹Natural means that it does not depend on a particular choice of coordinates.

where $a, c \in \mathbb{R}^3$ correspond to $\hat{a}, \hat{c} \in so(3)$ as in Eq.(1). However, there only exists one choice (up to a coefficient, [1], [26], [5], [3]) when the metrics needs to be *bi-invariant* (i.e. both right- and left-invariant):

$$\langle\langle \hat{a}, \hat{c} \rangle\rangle_{so(3)} \triangleq a^T I c = a^T c = \langle a, c \rangle \quad (5)$$

where I is the 3×3 identity matrix.

Two main results provided in [5] are:

- the existence of a natural norm² on $SO(3)$:

$$\|R\|_{SO(3)} = \langle\langle \hat{\phi}_R, \hat{\phi}_R \rangle\rangle_{so(3)}^{1/2} = \|\phi_R\|_{\mathbb{R}^3} \quad (6)$$

- and a formula for computing its time derivative on the Lie algebra $so(3)$:

$$\frac{1}{2} \frac{d}{dt} \|R(t)\|_{SO(3)} = \langle\langle \hat{\phi}_R, R^T \dot{R} \rangle\rangle_{so(3)} \quad (7)$$

where $\hat{\phi}_R \in so(3)$, also referred to as $\log R$, is defined as the angular velocity that takes the rigid body from I to $R \in SO(3)$ in *one* time unit, see [26] for details on the *logarithmic map*:

$$\hat{\phi}_R = \log R = \frac{\theta_R}{2 \sin \theta_R} (R - R^T) \quad (8)$$

where, for $\text{trace}(R) \neq -1$, θ_R satisfies $1 + 2 \cos \theta_R = \text{trace}(R)$ and $\|\phi_R\|^2 = \theta_R^2$, and the *Rodrigues' formula*:

$$R = \exp(\hat{\phi}_R) = I + \alpha_R \hat{\phi}_R + \beta_R \hat{\phi}_R^2 \quad (9)$$

where $\alpha_R = \|\phi_R\|^{-1} \sin \|\phi_R\|$ and $\beta_R = (1 - \cos \|\phi_R\|) \|\phi_R\|^{-2}$.

III. MICROMECHANICAL FLYING INSECT

In this section we review the most important features of a Micromechanical Flying Insect, summarizing some of the results presented in [10][11].

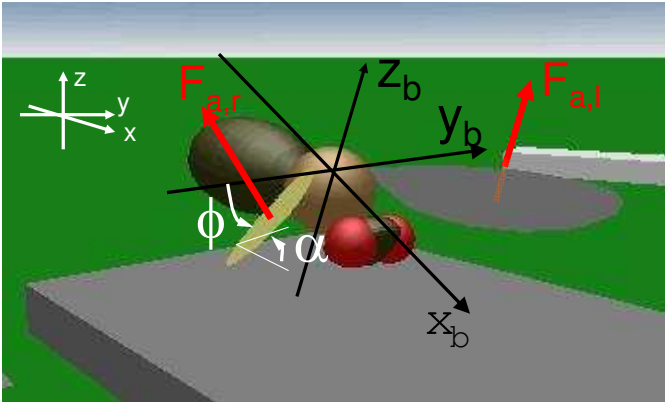


Fig. 1. Insect showing the equivalent instantaneous aerodynamic forces acting on each wing, the stroke angle ϕ and the angle of attack α .

A. Flying Insect Dynamics

Insect flight dynamics is still a very active area of research. In particular, there is great interest in understanding the unsteady state nature of flapping wings aerodynamics, which is believed to be source of the high maneuverability of insect flight as compared to fixed-winged vehicles and helicopters [30]. A detailed discussion of flying insect aerodynamics and modeling is beyond the scope of this paper, and we address the interested readers to the recent paper by Deng *et al.* and references therein [10]. Here, we simply summarize some results relevant to our discussion.

Since the mass of the wings is negligible with respect to the body mass, the dynamics of a flying insect can be modeled as the dynamics of a rigid body subject to external forces and torques:

$$J \dot{\omega}_b = \tau_b - \omega_b \times J \omega_b \quad (10)$$

$$m \dot{v}_b = f_b - \omega_b \times m v_b \quad (11)$$

where m and J are the insect mass and moment of inertia, respectively, and τ_b and f_b are the total external torque and force computed with respect to the insect center of mass in the body frame. The external force and torques are due to the gravity, insect body drag and wings aerodynamic forces:

$$\tau_b = \tau_{aero} \quad (12)$$

$$f_b = -b v_b - R^T f_g + f_{aero} \quad (13)$$

where R is the rotation matrix from body frame to fixed frame, $f_g = [0 \ 0 \ -mg]^T$ is the gravitational force, b is a damping coefficient, and τ_{aero}, f_{aero} are due to the aerodynamic forces generated by the flapping wings. These toques and moments are highly time-varying functions of the two wings kinematics:

$$\tau_{aero} = \tau_{aero}(\phi_r, \phi_l, \alpha_r, \alpha_l, \dot{\phi}_r, \dot{\phi}_l, \dot{\alpha}_r, \dot{\alpha}_l)$$

$$f_{aero} = f_{aero}(\phi_r, \phi_l, \alpha_r, \alpha_l, \dot{\phi}_r, \dot{\phi}_l, \dot{\alpha}_r, \dot{\alpha}_l)$$

where ϕ and α are the stroke angle and the angle of attack of one wing, respectively, as shown in Fig. 1 and the subscripts r, l stand for right and left wing. The exact dependence of the torque and force on the wings kinematics is very complex. However, in [11] it was suggested to parameterize the wings kinematics according to some parameters inspired by observation of real insects as follows:

$$\phi_r = h_1(v, t)$$

$$\phi_l = h_2(v, t)$$

$$\alpha_r = h_3(v, t)$$

$$\alpha_l = h_4(v, t)$$

where $v = [v_1 \dots v_5]^T$ is the vector of kinematics parameters like stroke angle offset and relative difference between upstroke and downstroke angle of attack, and h_i are T-periodic function in t , where T is wingbeat period. According to this parametrization it was shown that the forces and torques acting

²Which measures the distance between R and the identity I .

on the inset center of mass can be written as

$$\begin{aligned}\tau_{aero} &= \begin{bmatrix} u_1(v) \\ u_2(v) \\ u_3(v) \end{bmatrix} + \begin{bmatrix} \tilde{\tau}_x(t) \\ \tilde{\tau}_y(t) \\ \tilde{\tau}_z(t) \end{bmatrix} \\ f_{aero} &= \begin{bmatrix} 0 \\ 0 \\ mg \end{bmatrix} + \begin{bmatrix} u_4(v) \\ 0 \\ u_5(v) \end{bmatrix} + \begin{bmatrix} \tilde{f}_x(t) \\ \tilde{f}_y(t) \\ \tilde{f}_z(t) \end{bmatrix}\end{aligned}$$

where $u = [u_1 \dots u_5]^T$ is the vector of virtual input, and $\tilde{f}_x(t), \dots, \tilde{\tau}_z(t)$ are all T-periodic functions with zero-mean. It was also shown that the map from wing kinematics parameter v to the virtual input parameters u is invertible and linearizable, i.e.

$$u = Tv \quad (14)$$

where $T \in \mathbb{R}^5$ is invertible, i.e. $v = T^{-1}u$. From averaging theory arguments, the time varying components of the force and torques can be neglected, therefore it is possible to implicitly assume that the torque and the x and z components of the body force can be controlled independently [11]. In particular, we can rewrite (10) as:

$$J\dot{\omega} = \tau_u - \omega \times J\omega \quad (15)$$

where $\tau_u \in \mathbb{R}^3$ is the controllable torque input vector, and we dropped the subscript b to simplify notation. In the rest of the paper the angular velocity ω is to be intended with respect to the body frame unless differently stated.

B. Sensory System

Another reason for superior performance exhibited by flying insects, besides the enhanced unsteady state aerodynamic forces from flapping flight, is the highly specialized sensory system. In order to stabilize flight, insects can rely upon a number of different sensors. In the following, we briefly review a number of sensors available to insects for navigation, which represent a rich source of inspiration for the mechanical flying insect [7], [10].

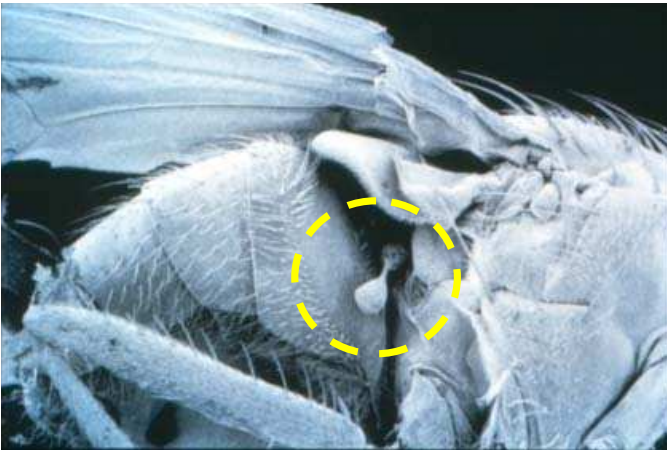


Fig. 2. Photo of a fly haltere. Courtesy of [8].

1) *Halteres*: The halteres are club-shaped small appendages behind each wing that oscillate in anti-phase with respect of

the wing, as shown in Fig. 2. The plane of oscillation is slightly tilted toward the tail of the insect to be able to measure Coriolis forces along all three body axes [17]. The halteres function as tiny gyroscopes and through appropriate signal processing [27] they can reconstruct the body angular velocity vector:

$$y_{hl} = \omega \quad (16)$$

The major drawback of halteres is that their measurements can be unpaired by body translational acceleration, which cannot be distinguished from the Coriolis forces. However, this problem can be alleviated by integrating angular velocities estimates from sensors such as the ocelli and the compound eyes visual system, which are immune from linear accelerations. Recently, preliminary prototypes of micro-electromechanical halteres have been fabricated and have shown promising results [38].

2) *Mechanoreceptors*: Insects wings and other parts of the body such as the antennae, neck and legs are innervated by campaniform sensilla. These nerves can sense and encode pressure forces when they are stretched or strained [12]. A large number of sensilla are located at the base of the wing to measure aerodynamic forces acting on the wings during motion and to elicit a compensatory mechanism to stabilize wing trajectory. Differently, the sensilla on the legs can be used to measure the gravity sensor, thus acting as a gravimeter. Therefore, we can assume that insect can measure the gravity vector with respect to the body frame, i.e.

$$y_g = R^T g_0 \quad (17)$$

where g_0 are the (known) gravity vector components, measured with respect to the fixed frame. Similarly to the halteres, also the mechanoreceptors are affected by linear body accelerations, and need to be integrated with other sensors.

3) *Ocelli*: The ocelli are three additional light-sensitive organs that look forward, leftward and rightward, respectively, located in the middle of the compound eyes as shown in Fig. 3 and provide signals that are used for stabilization with respect to rapid perturbations in roll and pitch [7]. In fact, these sensor can estimate the position of the sun with respect to insect body by comparing the signals from the left and right ocelli to estimate the roll angle, and by comparing the signal from the forward-looking ocellus with the mean of the signals from the left and the right ocelli to estimate the pitch angle [33].

4) *Compound eyes*: The compound eyes of the insects provides different types of signals needed for the optomotor systems. They provide computation of insect angular velocities accomplished by using large-field neurons that are tuned to respond to the specific patterns of optic flow that are generated by yaw, roll and pitch [28]. Differently from halteres, these estimates requires longer signal processing periods, but are not affected by linear accelerations. In other words, compound eyes precisely estimate angular velocities at low frequencies.

The compound eyes can also estimate body orientation and position by higher level visual processing like object fixation and landmarks detection. Although this signal processing requires even longer times, it can provide useful position information at low frequency for navigation and path planning [13].

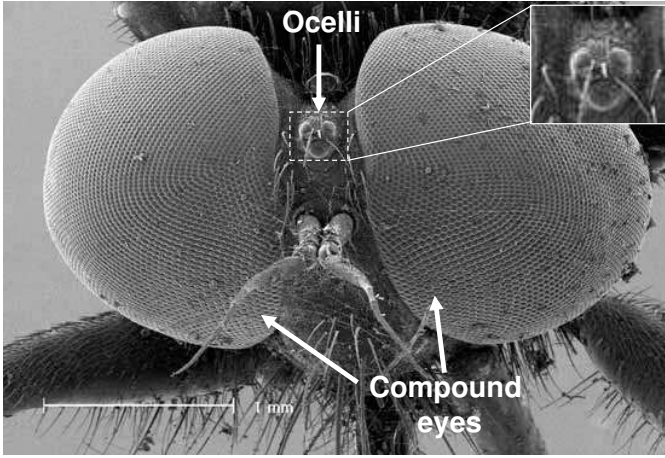


Fig. 3. Photo of fly's head showing compound eyes and the ocelli with its three photoreceptors. Courtesy of [35].

Finally, the dorsally directed (upward-looking) regions of the compound eyes of many insects are equipped with specialized photoreceptors that are sensitive to the polarized light patterns that are created by the sun in the sky. These photoreceptors feed into polarization-sensitive interneurons that function as “celestial compasses”, informing the insect about the direction in which it is flying in relation to the sky's polarization pattern. The polarization-sensitive system is used by insects to establish and maintain the correct heading direction whilst navigating toward a distant goal. In other words, insects can measure their orientation relative to the direction of the light polarization: $p_0 \in \mathbb{R}^3$, as:

$$y_p = R^T p_0 \quad (18)$$

Differently from the ocelli, the light polarization direction is not affected by light intensity. In fact, while estimation of sun position using the ocelli can be unpaired when passing from a shaded region to a sunny region, the estimation of polarization direction is unaffected. Bio-inspired polarized light compasses have been successfully fabricated and used for robot navigation [22].

5) *Magnetic compass*: Recent studies indicate that some insects also possess a magnetic sense that informs them of their heading direction, and helps them maintain it [36]. Similarly to the light polarization sensor, we can argue that insect can measure the components of the magnetic field with respect to the body as follows:

$$y_m = R^T b_0 \quad (19)$$

where $b_0 \in \mathbb{R}^3$ is the direction of magnetic field relative to the fixed frame. A possible electromechanical implementation of a magnetic compass suitable for small size vehicles is given in [39].

IV. SENSOR FUSION VIA COMPLEMENTARY FILTERS

The sensory system of real insects is clearly redundant, i.e. kinematic quantities such as the angular velocity are derived from more than one sensor. Information from different sensors is then “fused” together.

Complementary filters traditionally arise in applications where redundant measurements of the same signal are available [2] and the problem is combining all available information in order to minimize the instrumentation error.

For sake of simplicity, consider only two sensors, s_1 and s_2 , providing readings of the *same* quantity, e.g. the angular velocity ω , with different noise characteristics, i.e. $s_1 = \omega + n_1$ and $s_2 = \omega + n_2$, where $\|n_1\| < \|n_2\|$ at high frequency while $\|n_2\| < \|n_1\|$ at low frequency.

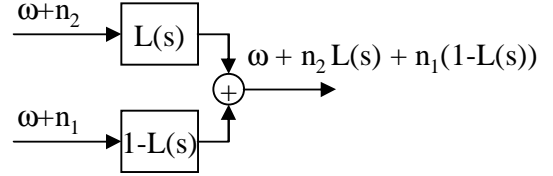


Fig. 4. Sensor fusion via a complementary filter. The low-pass is $L(s)$ while the high-pass is defined as $1-L(s)$, in this sense the filter is “complementary”.

Complementary filters such as the one in Fig. 4 can be used to fuse information from two or more sensors (e.g. halteres, ocelli and compound eyes) with the characteristic of sensing the *same* variable (e.g. angular velocity) although being subject to noise and disturbances with different spectral content [2].

Remark 1 (non-dynamic estimation): The kinematic variable (ω in Fig. 4) is dynamically *unaffected* by the filter. The estimated variable (i.e. the output of the filter) is related to the input variable via a purely algebraic relation in the time domain and no dynamics are involved in the noiseless case.

Such filters can be safely used in feedback loops to fuse readings of the *same* kinematic variable from different sensors since no extra dynamics is added to the overall system and stability (which involves noiseless conditions) is not affected.

Complementary filters can be generalized to fuse information deriving from sensors when the sensed variables are related by differential equations, i.e. the filter introduces some dynamics between the estimated output and the sensed inputs.

The differential equations relating the sensed variables may be nonlinear, this is typically the case when attitude is concerned. Theory of complementary and Kalman filters has been traditionally been used to design attitude filters. Although the Kalman filters can be extended (EKF) to nonlinear cases, they fail in capturing the nonlinear structure of the configuration space of problems involving, for example, rotations of a rigid body, and most importantly, they can run into instabilities. On the other hand, nonlinear filters [9], in particular complementary filters, can better capture such a nonlinear structure.

A. Dynamic Attitude Estimation

As an example of use of complementary filters when *different* kinematic variables are involved, consider the linear case of a rotational mechanical system with one degree of freedom (θ). As shown in [2], complementary filters such as the one represented in Fig. 5 are traditionally used to fuse information available from both angular position sensors and tachometers, respectively θ_{sens} and ω_{tacho} . Let θ^* be the estimate of θ .

The filter gain k in Fig. 5 determines the transition frequency of the filter after which the data from the tachometer (ω_{tacho}) are weighted more whereas before the transition frequency data from the position sensors (θ_{sens}) are predominant on the dynamic equation (the integrator $1/s$). The optimal value for k is in fact determined by the characteristics of measurement noise, see [2].

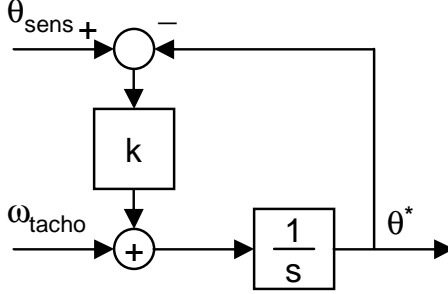


Fig. 5. Linear complementary filter for a rotational mechanical system with one degree of freedom.

Differently from previous example, $SO(3)$ is a *nonlinear* space and that is where the advantages of a geometric approach can be fully appreciated. Besides nonlinear dynamics, the very definition of estimation error requires caution. In the linear case $e = \theta - \theta^*$ is a typical choice while quantities such as $R - R^*$ with $R, R^* \in SO(3)$ are no longer guaranteed to belong to $SO(3)$. Following [5], the estimation error will be defined in (22) as $E = R^T R^*$.

Next, a complementary filter on $SO(3)$ for dynamic attitude estimation is presented which fuses information from gyroscopes and from different and possibly redundant navigation sensors, such as the ones described in Section III.

B. Complementary filtering on $SO(3)$

Consider $N \geq 2$ homogenous and time-invariant vector fields $\vec{v}_1, \vec{v}_2, \dots, \vec{v}_N$ (e.g. the gravitational field, the geomagnetic field, the light direction etc...) without the need, for the moment, to specify their components (therefore the symbol $\vec{\cdot}$). Assume that at least two of them (e. g. \vec{v}_1 and \vec{v}_2 , without loss of generality) are independent, this can be expressed in a form that is invariant and coordinate-free:

$$\vec{v}_1 \times \vec{v}_2 \neq 0 \quad (20)$$

Definition 1: Given a rigid body, define a body frame \mathcal{B} on it. Let the rigid body be at rest at some time t_0 and define thus a space frame S_0 as the one coincident with the body frame \mathcal{B} at time t_0 . Let the constant vectors $v_{i0} = [v_{i0x} \ v_{i0y} \ v_{i0z}]^T$ represent the components of each vector field at time t_0 as measured by a set of sensors on the rigid body. At any time t , let $R(t) : \mathbb{R} \rightarrow SO(3)$ be a twice-differentiable function representing the orientation of the rigid body in 3D space with respect to the space frame S_0 , let $v_i = [v_{ix} \ v_{iy} \ v_{iz}]^T$ be the (time-variant) components of each field and let ω_{gyr} be readouts of the gyroscopes, both v_i and ω_{gyr} are referred to the (body) moving frame.

Before presenting the main theorem concerning the proposed observer and its convergence properties, two lemmas

are presented which relate the influence of the current attitude R on the sensor measurements v_i as well as the role of gyroscopes in navigation.

Lemma 1: The trajectory $R(t) \in SO(3)$, defined as in Definition 1, is reflected in the measurements of the gyroscopes and of the vector fields sensors and can be expressed as

$$\begin{cases} \hat{\omega}_{gyr} &= R^T \dot{R} = \hat{\omega} \\ v_i &= R^T v_{0i} \end{cases} \quad (21)$$

See proof in Appendix II.

Lemma 2: Let $R(t) : \mathbb{R} \rightarrow SO(3)$ represent, as in Definition 1, the trajectory on $SO(3)$ of a rigid body embedding a set of gyroscopes and let the angular velocity ω of the rigid body be available, as in (21), via readings from such gyroscopes. Let $R^{*T} \dot{R}^* = \hat{\omega}$ denote the dynamics of an estimator, then the tracking error

$$E \triangleq R^T R^* \quad (22)$$

is such that $\|E(t)\|_{SO(3)} = \text{constant}$. In particular, the following identity holds:

$$\langle \langle \log(E), -E^T \hat{\omega} E + \hat{\omega} \rangle \rangle_{so(3)} = 0 \quad (23)$$

See proof in Appendix II.

Theorem 1: Let $R(t) : \mathbb{R} \rightarrow SO(3)$ represent the orientation of the rigid body as in Definition 1. Let $R^*(t)$ denote the estimate of $R(t)$ and let it be defined by the following observer:

$$\begin{cases} \dot{R}^* &= R^* \hat{\omega}^* \\ \omega^* &= \omega_{gyr} + \sum_{i=1}^N k_i (v_i \times v_i^*) \\ v_i^* &= R^{*T} v_{0i} \end{cases} \quad (24)$$

where $k_i > 0$ are the filter gains, ω_{gyr} and v_i represent the sensor readings as in (21).

The observer (24) asymptotically tracks $R(t)$ for almost any initial condition $R^*(0) \neq R(0)$ and in particular:

$$\lim_{t \rightarrow \infty} R^T(t) R^*(t) = I \quad (25)$$

See proof in Appendix II.

Besides proving almost-global asymptotic stability of the proposed observer (24), Theorem 1 also provides an upper bound of the attitude tracking error dynamics which shall be used later. Following [5], a natural³ Lyapunov function of the tracking error $E = R^T R^*$ is chosen to be

$$W(E) = \frac{1}{2} \|E\|_{SO(3)}^2 = \frac{1}{2} \|\phi_E\|^2 \quad (26)$$

where ϕ_E is defined via (8) as $\hat{\phi}_E = \log E$.

In particular, Theorem 1 proves that there exists $\eta > 0$ such that, if the initial estimation error $E(0)$ is such that $\text{trace} E \neq -1$ (i.e. $\|\phi_E\| < \pi$ which is *almost* globally verified, see Remark 2 below), then a bound for the Lyapunov function is

$$0 < W(E) < W(E(0)) e^{-\eta t}$$

³based on the natural norm (6) on $SO(3)$

for all $t > 0$. This translates, via the (26), into an upper bound for the attitude tracking error:

$$\|\phi_E\| < c\|\phi_E(0)\|e^{-\lambda t} \quad (27)$$

where $c = W(E(0))/\|\phi_E(0)\|$ and $\lambda = \eta/2$.

This satisfies assumption A.2 of Lemma 3 in the appendix.

Remark 2 (π -rotations): The chosen Lyapunov function (26) proves convergence *almost* for all possible initial estimation errors $E(0)$. A question arises: *what can be said about the initial configurations which are left out?* Note first that, as clear from the definition of the logarithmic map in (8), *any* configuration can be reached via a rotation about some axis by an angle less than or equal⁴ to π . The only configurations left out by the chosen Lyapunov function are those such that $\text{trace}(E) \neq -1$, i.e. such that $\|\phi_E\| = \pi$. Such configurations correspond to the set of rotations about an arbitrary axis by an angle exactly equal to π and will be referred to as π -rotations.

Consider the typical case where only the gravitational (v_1) and the geomagnetic (v_2) fields are involved. Consider a rotation R_π of π radians about an axis perpendicular to the plane containing both the gravity vector v_1 and the geomagnetic vector v_2 . It's straightforward verifying that $R_\pi v_1 = -v_1$ and that $R_\pi v_2 = -v_2$ and that the correction terms for the observer are zero, i.e. R_π is an equilibrium (of course an unstable one). There also exist other unstable equilibria among the π -rotations, some of which depend also on the values of k_1 and k_2 .

Remark 3 (unstable equilibria): The presence of unstable equilibria among the π -rotations excludes the possibility of a better choice for the Lyapunov function. In practice, unstable equilibria do not represent an issue due to the presence of noise.

C. Filter Implementation

In this section, the implementation for the specific case of two vector fields $v_1 = g$ and $v_2 = b$, with setup measurements $v_{01} = g_0$ and $v_{02} = b_0$, together with data from gyroscopes (ω_{gyr}), is presented. In particular, Fig. 6 shows the general observer (24) in terms of block diagrams which can be directly implemented in simulation environments such as MATLAB/Simulink from MathWorks Inc.

The diagram in Fig. 6, in particular the integration block $1/s$, is a continuous-time filter. Any digital implementation of the filter would *i*) transform the filter in a discrete-time one with time sequence t_n and *ii*) necessarily introduce numerical errors. The main risk is that, as numerical errors accumulate, quantities such as $R_n^* = R^*(t_n)$ are likely to *drift away* from $SO(3)$, i.e. $\det R_n^*$ very different from 1 and/or $R_n^{*T} R_n^*$ very different from the identity matrix I . This can be avoided by considering that data from analog sensors are typically acquired via DACs (Digital to Analog Converters) with a fixed sampling time, let this sampling time be ΔT . In the time interval $t_n \leq t < t_{n+1} = t_n + \Delta T$, data from sensors are assumed constant, i.e. $\omega(t) = \omega_n$, $g(t) = g_n$ and $b(t) = b_n$.

⁴Referring to the proof in Appendix II, π^2 in Fig. 8 represents the upper limit for the domain of \hat{W} .

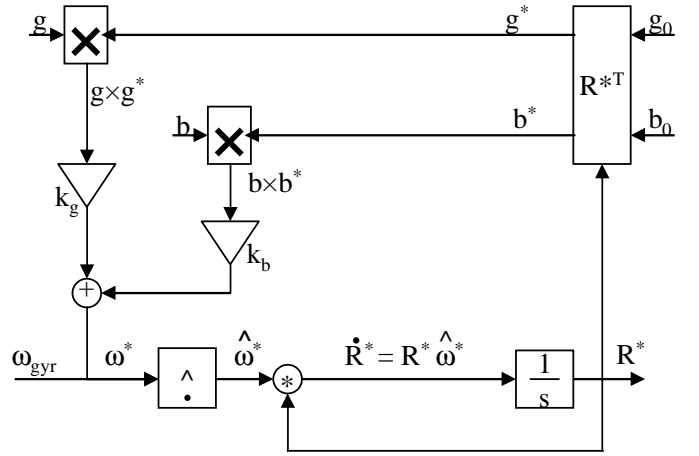


Fig. 6. Complementary filter for dynamic attitude estimation.

This allows computing R_{n+1}^* via the Rodrigues' formula (9) as:

$$\begin{aligned} \omega_n^* &= \omega_n + k_b(g_n \times (R_n^{*T} g_0)) + k_b(b_n \times (R_n^{*T} b_0)) \\ \alpha_n &= \sin \|\Delta T \hat{\omega}_n^*\| / \|\Delta T \hat{\omega}_n^*\| \\ \beta_n &= (1 - \cos \|\Delta T \hat{\omega}_n^*\|) / \|\Delta T \hat{\omega}_n^*\|^2 \\ R_{n+1}^* &= R_n^* (I + \alpha_n \Delta T \hat{\omega}_n^* + \beta_n \Delta T \hat{\omega}_n^{*2}) \end{aligned} \quad (28)$$

which is guaranteed *not* to drift away from $SO(3)$.

Remark 4 (sensor fusion on the Lie algebra): in linear cases as in Fig. 5, all the variables belong to the same space \mathbb{R}^n while, in the nonlinear filter in Fig. 6, variables in different nodes of the block diagram belong to very different spaces, some linear ($so(3)$) and some nonlinear ($SO(3)$). Sensor fusion *naturally* occurs on the linear space of angular velocities, i.e. the Lie algebra $so(3)$.

V. ATTITUDE STABILIZATION

Attitude dynamics of a mechanical flying insect are described by the system

$$\begin{cases} \dot{R} = R \hat{\omega} \\ \dot{\omega} = J^{-1}(J\omega \times \omega + \tau_{FB}(R, \omega)) \end{cases} \quad (29)$$

where the state (R, ω) is an element of the product space $SO(3) \times so(3)$.

In what follows, results of traditional attitude control, based on state feedback, is combined with the dynamic attitude observer presented in the previous section.

A. Attitude Control via State Feedback

Traditionally, control of (29) is performed via passivity-based arguments. Maithripala *et al.* [24] show that the system (29) can be stabilized by a state feedback (torque) $\tau_{FB}(R, \omega)$ which consists of a conservative part, derived from a potential (also referred to as “error”) Morse⁵ function $U : SO(3) \rightarrow \mathbb{R}$, and a dissipative (Rayleigh-type) part:

$$\tau_{FB}(R, \omega) = -J (R^T \text{grad}U + k_\omega \hat{\omega})^\vee \quad (30)$$

⁵A Morse function is function whose critical points are non-degenerate [3].

where $\text{grad}U$, the *gradient* of the function $U(R)$, is defined by the equalities

$$\begin{aligned}\dot{U}(R) &= \langle dU, R\hat{\omega} \rangle \\ &= \langle R^T dU, \hat{\omega} \rangle \\ &= \langle \langle R^T \text{grad}U, \hat{\omega} \rangle \rangle_{so(3)}\end{aligned}\quad (31)$$

Therefore, the problem of stabilizing (29) is reduced to defining a potential function $U(R)$ on $SO(3)$ with a nondegenerate critical point in the desired configuration $\bar{R} \in SO(3)$.

To this end, a commonly used potential function, first introduced by Koditschek in [21], on $SO(3)$ is:

$$U(R) \triangleq \frac{1}{2} \text{trace}(K(I - \bar{R}^T R)) \quad (32)$$

where K is a symmetric 3×3 matrix with eigenvalues $\{k_1, k_2, k_3\}$. Once the potential function $U(R)$ is defined, the gradient (and therefore the feedback torque) can be computed as in [4] via the time derivative of the error function:

$$\begin{aligned}\dot{U}(R) &= \frac{1}{2} \text{trace}(K(-\bar{R}^T \dot{R})) \\ &= \frac{1}{2} \text{trace}(-K \bar{R}^T R \hat{\omega}) \\ &= \frac{1}{2} \text{trace}(\text{skew}(K \bar{R}^T R)^T \hat{\omega}) \\ &= \langle \text{skew}(K \bar{R}^T R), \hat{\omega} \rangle\end{aligned}\quad (33)$$

where $\text{skew}(A) = \frac{1}{2}(A - A^T)$. This allows computing $R^T \text{grad}U$ via its definition in (31):

$$R^T \text{grad}U = J^{-1} \text{skew}(K \bar{R}^T R) \quad (34)$$

Convergence properties of systems like (29) when the state feedback (30) is used can be found in [24], [23], here briefly restated for the case of interest. The proof is based on La Salle's principle [31] and involves a function $V = U(R) + \frac{1}{2} \langle \hat{\omega}, \hat{\omega} \rangle_{so(3)}$ as well as a set $S \subset SO(3) \times so(3)$ defined as $S = \{(R, \omega) | \dot{V} = 0\}$.

The sign of \dot{V} is studied as follows:

$$\begin{aligned}\dot{V} &= \dot{U}(R) + \frac{1}{2} \dot{\omega}^T J \omega + \frac{1}{2} \omega^T J \dot{\omega} \\ &= \dot{U}(R) + \omega^T J \dot{\omega} \\ &= \dot{U}(R) + \omega^T (J \omega \times \omega + \tau_{FB}) \\ &= \dot{U}(R) + \omega^T \tau_{FB} \\ &= \dot{U}(R) + \langle \langle J^{-1} \tau_{FB}, \hat{\omega} \rangle \rangle_{so(3)}\end{aligned}\quad (35)$$

since $\omega^T (J \omega \times \omega) = 0$ for all $\omega \in \mathbb{R}^3$.

Considering (31) and (30), then:

$$\begin{aligned}\dot{V} &= \langle \langle R^T \text{grad}U, \hat{\omega} \rangle \rangle_{so(3)} + \langle \langle J^{-1} \tau_{FB}, \hat{\omega} \rangle \rangle_{so(3)} \\ &= -k_\omega \|\omega\|^2\end{aligned}\quad (36)$$

which implies $S = \{(R, \omega) | \omega = 0\}$ and

$$\langle \langle R^T \text{grad}U, \hat{\omega} \rangle \rangle_{so(3)} + \langle \langle J^{-1} \tau_{FB}, \hat{\omega} \rangle \rangle_{so(3)} \leq 0 \quad (37)$$

where the inequality is *strict* for all $(R, \omega) \notin S$, implying *asymptotic* convergence. This satisfies the assumption A.1 of Lemma 3 in the appendix.

In order to perform attitude stabilization of the system (29) via state feedback (30), the current attitude R and angular velocity ω need to be available.

Angular velocity can be directly measured from gyroscopes (for example fusing signals from halteres, ocelli and compound eyes by means of filters such as the one in Fig. 4) while attitude can be estimated from mechanoreceptors and magnetic

compass sensors, as shown next. This kind estimation is based on direct measurement and is therefore referred to as *non-dynamic* attitude estimation. As shown later, disturbances directly affect non-dynamic estimation resulting in a much less robust attitude stabilization.

B. Non-Dynamic Attitude Estimation Feedback

Attitude can be estimated via direct measurements of vector fields which are fixed with respect to the space frame, e.g. the gravity vector field, the geomagnetic vector field or the sun direction. The minimum number of independent vectors is two, e.g. gravity g and geomagnetic b vectors. If at time t_0 the body frame is aligned with the space frame, then $R(0) = I$ and define $g_0 = [g_{01} \ g_{02} \ g_{03}]^T$ and $b_0 = [b_{01} \ b_{02} \ b_{03}]^T$ respectively the gravity and the geomagnetic readings at time t_0 .

At any later time t , the body frame and the space frame are no longer necessarily aligned, i.e. the two frames can be related to one another via the orientation matrix $R(t)$ to be estimated. If $g = [g_1 \ g_2 \ g_3]^T$ and $b = [b_1 \ b_2 \ b_3]^T$ are the sensor readings for, respectively, the gravitational and the geomagnetic vector at time t , then the following relations hold:

$$g = R^T g_0; \quad b = R^T b_0 \quad h = R^T h_0 \quad (38)$$

where the vectors $h = [h_1 \ h_2 \ h_3]^T$ and $h_0 = [h_{01} \ h_{02} \ h_{03}]^T$ are conveniently defined as $h = g \times b$ and $h_0 = g_0 \times b_0$. Then the rotation matrix R can be evaluated from initial and current measurements as:

$$R = \begin{bmatrix} g_{01} & b_{01} & h_{01} \\ g_{02} & b_{02} & h_{02} \\ g_{03} & b_{03} & h_{03} \end{bmatrix} \begin{bmatrix} g_1 & b_1 & h_1 \\ g_2 & b_2 & h_2 \\ g_3 & b_3 & h_3 \end{bmatrix}^{-1} \quad (39)$$

It's worth noting that, unless very large (and unlikely) disturbances are present in the measurements, g and b are independent and, given the definition of h , the matrix inversion in (39) is always possible.

Remark 5: The matrix R evaluated via (39) is *not* guaranteed to be in $SO(3)$ unless measurements are error free. Some sort of "normalization" is necessary, i.e. a matrix $R^0 \in SO(3)$ should be found that is in some sense "close" to the result of (39). This normalization is typically done once a parameterization is chosen, e.g. quaternions, but it is arbitrary since it depends on parameterization itself.

These problems do not arise when the feedback (30) can be written explicitly in terms of measurements. A computation-ally convenient feedback law is

$$\tau_{FB}(R, \omega) = -J(k_g(g \times g_0) + k_b(b \times b_0) + k_\omega \omega) \quad (40)$$

where $k_\omega \omega$ represents the Rayleigh-type dissipative term, while the remaining part is a conservative term, i.e. τ_{FB} is in the form (30) which guarantees stability. It is straightforward verifying that such a conservative term derives from the following potential

$$\begin{aligned}U(R) &= -k_g \langle \langle g, g_0 \rangle \rangle - k_b \langle \langle b, b_0 \rangle \rangle \\ &= -k_g g_0^T R g_0 - k_b b_0^T R b_0\end{aligned}$$

where $\langle \langle a, b \rangle \rangle = a^T b$ is the dot product in \mathbb{R}^3 .

Remark 6: Feedback laws such as (30) and in particular (40) are directly affected by disturbances present in the measurements and rigid body dynamics may be largely influenced by such disturbances, depending on the operating conditions. For example, estimates such as (39) are reliable at low frequencies but *not* at high frequencies where non-inertial accelerations largely affect the gravity sensors. In the next section, information from gyroscopes (reliable at high frequencies) is “fused” with information from magnetic and gravity sensors via a nonlinear complementary filter.

C. Dynamic Attitude Estimation Feedback

In this section, previous results on attitude control via state feedback and dynamic attitude estimation via nonlinear complementary filters are fused together by means of the “separation principle” in Lemma 3 in the appendix, reported from [24] for convenience.

The attitude control system comprising the dynamic state observer is described by

$$\begin{cases} \dot{R} = R\hat{\omega} \\ \dot{\omega} = J^{-1}(\tau_{FB}(R^*, \omega^*) - \omega \times J\omega) \\ \dot{R}^* = R^*\hat{\omega}^* \\ \omega^* = \omega_{gyr} + k_b(b \times b^*) + k_g(g \times g^*) \end{cases} \quad (41)$$

In order to apply the separation principle, rewrite (41) as

$$\begin{cases} \dot{R} = R\hat{\omega} \\ \dot{\omega} = J^{-1}(\tau_{FB}(R, \omega) - \omega \times J\omega) + \psi(R, \omega, q) \\ \dot{R}^* = R^*\hat{\omega}^* \\ \omega^* = \omega_{gyr} + k_b(b \times b^*) + k_g(g \times g^*) \end{cases} \quad (42)$$

where $\psi(R, \omega, q)$ represents the term $J^{-1}(\tau_{FB}(R^*, \omega^*) - \tau_{FB}(R, \omega))$. This is possible because ω^* is a (linear) function of R, ω and R^* . The estimate R^* can be written as $RR^T R^* = RE$ and E , the estimation error defined in (22), can be parameterized by $q \triangleq \phi_E$ ($E = \exp \hat{q}$) as in (48).

Since $\phi(R, \omega, q)$ is linear in ω and $SO(3)$ is a *compact* Lie group, then assumption A.3 of Lemma 3 in the appendix is automatically satisfied, see [23, Assumption 3] for details.

Recalling that also assumptions A.1 and A.2 in Lemma 3 where satisfied (respectively in (37) and (27)), then Lemma 3 guarantees that the system (41) *almost* globally stabilizes the attitude at $(\bar{R}, 0) \in SO(3) \times so(3)$ and that convergence is asymptotic.

VI. ROBUSTNESS: SIMULATION RESULTS

In this section, the difference between a non-dynamic state estimation and a dynamic observer in terms of robustness to disturbances is presented, in particular when the estimate is used for attitude stabilization.

As long as insects are concerned, a typical source of disturbance is represented by sudden gusts of wind. This situation can be modeled as a translation (due to the wind) of the insect body along some axis. Although purely translational, this disturbance also affects the attitude since non-inertial accelerations add up to the gravitational acceleration as this is sensed by mechanoreceptors, causing a misperception of the vertical axis and therefore an attitude estimation error.

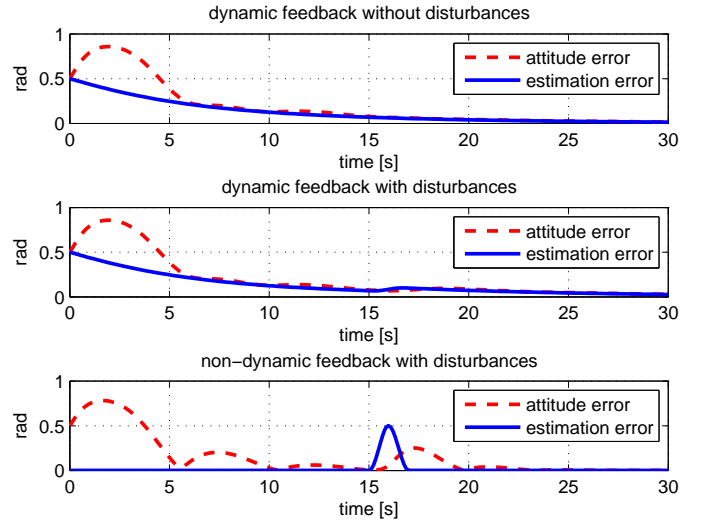


Fig. 7. Effect disturbances on attitude stabilization in the cases of dynamic and non-dynamic state feedback.

A wind gust is simulated to occur at time 15 seconds and to last for 2 seconds and the attitude and estimation errors (in radians, as in (6)) are considered. The wind gust, directly affects the non-dynamic estimation error in Fig. 7 (bottom), causing the stabilization control system to promptly react although there was no attitude error.

The dynamic observer in Fig. 7 (middle), if compared with case with no disturbances in Fig. 7 (top), has a “low-pass” behavior, i.e. rejects sudden changes from sensors, and the attitude control system is almost unaffected by the disturbance. It should be noticed how a “low-pass” behavior is present before the disturb is applied (0-15 seconds) where the observer exponentially recovers from an initial estimation error (purposely set as an initial condition).

In conclusion, although in the ideal case (before the wind gust at time 15 seconds) the non-dynamic state estimation displays no estimation error at all while the dynamic observer may take some time to settle down to zero estimation error (depending on the initial conditions), when disturbances arise, i.e. in practical conditions, the dynamic observer is more robust.

VII. CONCLUSION

In this work, we present a geometric, i.e. intrinsic and coordinate-free, approach to attitude stabilization of a micro-mechanical flying insect. Stabilization is achieved via traditional passivity-based attitude controllers where the state feedback is derived from multiple and possibly redundant bio-inspired navigation sensors.

Such a multimodal sensor fusion is implemented by a dynamic observer, in particular a complementary filter is proposed which is specialized to the nonlinear structure of the Lie group of rigid body rotations. Almost-global, asymptotic stability of the proposed filter is proved as well as stability of the overall system combining traditional attitude controllers and dynamic output from the proposed observer.

Finally, simulations are used to show the benefits of dynamic attitude estimation in terms of robustness to disturbances.

As future work, the effect of noise and disturbances, especially those due to self-motion, will be analyzed in terms of tracking accuracy. Based on this analysis, optimal criteria for tuning gains of complementary filters according to each specific operating conditions will be defined, a necessary step before proceeding to hardware implementation on a robotic platform.

ACKNOWLEDGEMENT

This work was partly supported by a grant from the European Union, FP6-NEST/Adventure Programme, contract no. 015636, and by a grant from ‘‘Regione Lazio’’ under the ‘‘DOCUP 2000/2006 - Sottomisura II.5.2 - progetto ITINERIS’’ Programme.

APPENDIX I SEPARATION PRINCIPLE

In this section the Lemma presented in [24, Corollary.2] and proved in [23] for a general Lie group G , is specifically rewritten for the case $G = SO(3)$. Consider the system

$$\begin{cases} \dot{R} = R\omega \\ \dot{\omega} = J^{-1}(J\omega \times \omega + \tau_{FB}(R, \omega)) + \psi(R, \omega, q) \end{cases} \quad (43)$$

with $(R, \hat{\omega}) \in SO(3) \times so(3)$ and $q \in \mathbb{R}^n$ and $V = U(R) + \frac{1}{2}\langle \hat{\omega}, \hat{\omega} \rangle_{so(3)}$, where $U(R)$ is a smooth globally defined Morse function representing the potential energy of the system. Also consider the following assumptions.

Assumption A.1: *The point $(\bar{R}, 0)$ is an almost globally stable equilibrium point of (43) with $\psi \equiv 0$ and furthermore*

$$\langle \langle R^T \text{grad } U, \hat{\omega} \rangle \rangle_{so(3)} + \langle \langle J^{-1} \hat{\tau}_{FB}, \hat{\omega} \rangle \rangle_{so(3)} \leq 0 \quad (44)$$

The condition (44) is satisfied by any simple⁶ mechanical system with potential energy $U(R)$ and Rayleigh-type dissipation. The equilibrium $(\bar{R}, 0)$ is an almost globally stable equilibrium if \bar{R} is a unique minimum of $U(R)$.

Assumption A.2: *The function $q(t) \in \mathbb{R}^n$ satisfies*

$$\|q(t)\| \leq c\|q(0)\|e^{-\lambda t} \quad (45)$$

for some $c > 0$, $\lambda > 0$, and all $t > 0$.

Assumption A.3: *The interconnection term satisfies $\psi(R, \omega, 0) \equiv 0$ and the linear growth conditions*

$$\|\psi\| \leq \gamma_1(\|q\|) \|\omega\| + \gamma_2(\|q\|) \quad (46)$$

for two \mathcal{K}_∞ functions $\gamma_1(\cdot)$, $\gamma_2(\cdot)$.

Lemma 3: *If the Lie group G is compact and if Assumptions A.1-A.3 are satisfied, then the equilibrium $(\bar{R}, 0)$ of the system (43) is almost-globally stable. Convergence is asymptotic if the inequality in Assumption A.1 is strict.*

⁶Simple mechanical systems are those mechanical systems (a large class) with a kinetic energy lagrangian and subject to a potential force, see [3].

APPENDIX II PROOFS OF MAIN THEOREM AND RELATED LEMMAS

Proof of Lemma 1:

Monoaxial sensors are characterized by a sensitive axis along which the components of a vector field (e.g. angular velocity, gravitational field, geomagnetic field etc...) can be measured. A body frame \mathcal{B} identifies three orthogonal directions on a rigid body. Monoaxial sensors are, by construction, assembled on a rigid body in such a way that their sensitive axis coincides with one of axes defined by \mathcal{B} .

By construction, a set of three monoaxial gyroscopes provides the components of the angular velocity with respect to the body frame \mathcal{B} , i.e. $\hat{\omega}_{gyr} = \hat{\omega} = R^T \dot{R}$.

As for the effect of an arbitrary rotation R on the components of the fields $\vec{v}_1, \vec{v}_2, \dots, \vec{v}_N$ as these are measured in the body frame, when the body frame coincides with the space frame \mathcal{S}_0 , by Definition 1, the fields components are given by v_{0i} both in the body frame and in the space frame, i.e. the identity matrix I relates the field components in \mathcal{S}_0 with the measured components in the body frame. For an arbitrary orientation R of the body with respect to \mathcal{S}_0 the components of the fields as measured by the sensors relative to the body can be expressed as $v_i = R^T v_{0i}$. ■

Proof of Lemma 2:

First, a proof of (23) is provided which mainly makes use of the following identities on $so(3)$ which hold for all $x, y \in \mathbb{R}^3$:

$$\begin{aligned} \hat{x} &= -\hat{x}^T \\ \hat{x}^2 &= \hat{x}^{2T} \\ \hat{x}\hat{y} &= yx^T - x^T y I \\ \widehat{\hat{x}\hat{y} - \hat{y}\hat{x}} &= \widehat{(x \times y)} \\ \widehat{\hat{x}\hat{y}^2 + \hat{y}^2\hat{x}} &= -\|y\|^2 \hat{x} - x^T y \hat{y} \\ \widehat{\hat{x}\hat{y}\hat{x}} &= -x^T y \hat{x} \\ \widehat{\hat{x}^2\hat{y}\hat{x} - \hat{x}\hat{y}\hat{x}^2} &= 0 \\ \widehat{\hat{x}^2\hat{y}\hat{x}^2} &= x^T y \|x\|^2 \hat{x} \end{aligned} \quad (47)$$

where $x^T y$ is the dot product in \mathbb{R}^3 .

Express E as a function of ϕ_E (where $\hat{\phi}_E = \log(E)$) via the Rodrigues' formula (9):

$$E = \exp(\hat{\phi}_E) = I + \alpha_E \hat{\phi}_E + \beta_E \hat{\phi}_E^2 \quad (48)$$

$$\text{where } \begin{cases} \alpha_E &= \frac{\sin \|\phi_E\|}{\|\phi_E\|} \\ \beta_E &= \frac{1 - \cos \|\phi_E\|}{\|\phi_E\|^2} \end{cases} \quad (49)$$

Using identities (47) and the fact that $\beta_E - \alpha_E^2 - \beta_E^2 \|\phi_E\|^2 = -\beta_E$, expand the term $-E^T \hat{\omega} E + \hat{\omega}$ after substituting (48) as:

$$\begin{aligned} -E^T \hat{\omega} E + \hat{\omega} &= \alpha_E (\widehat{\phi_E \times \omega}) + \beta_E \|\phi_E\|^2 \hat{\omega} + \\ &\quad + \phi_E^T \omega (\beta_E - \alpha_E^2 - \beta_E^2 \|\phi_E\|^2) \hat{\phi}_E \\ &= \alpha_E (\widehat{\phi_E \times \omega}) + \\ &\quad + \beta_E \|\phi_E\|^2 \hat{\omega} - \beta_E (\phi_E^T \omega) \hat{\phi}_E \end{aligned}$$

It is now straightforward verifying equation (50) (on top of next page) which proves (23).

Given the tracking error definition $E = R^T R^*$, the error dynamics are easily computed as

$$\dot{E} = \dot{R}^T R^* + R^T \dot{R}^*$$

$$\begin{aligned}
\langle \langle \log(E), -E^T \widehat{\omega} E + \widehat{\omega} \rangle \rangle_{so(3)} &= \langle \langle \widehat{\phi}_E, \alpha_E (\widehat{\phi}_E \times \omega) + \beta_E \|\phi_E\|^2 \widehat{\omega} - \beta_E (\phi_E^T \omega) \widehat{\phi}_E \rangle \rangle_{so(3)} \\
&= \phi_E^T (\alpha_E (\phi_E \times \omega) + \beta_E \|\phi_E\|^2 \omega - \beta_E (\phi_E^T \omega) \phi_E) \\
&= 0 + \beta_E \|\phi_E\|^2 (\phi_E^T \omega) - \beta_E (\phi_E^T \omega) \|\phi_E\|^2 \\
&= 0
\end{aligned} \tag{50}$$

Since $R^{*T} \dot{R}^* = \widehat{\omega} = R^T \dot{R}$, it can be verified that

$$E^T \dot{E} = -E^T \widehat{\omega} E + \widehat{\omega}$$

Rather than $E(t)$, we are interested in $\|E(t)\|$ and from (7) we can write:

$$\begin{aligned}
\frac{d}{dt} \|E(t)\|_{SO(3)} &= \langle \langle \widehat{\phi}_E, E^T \dot{E} \rangle \rangle_{so(3)} \\
&= \langle \langle \widehat{\phi}_E, -E^T \widehat{\omega} E + \widehat{\omega} \rangle \rangle_{so(3)} \\
&= 0
\end{aligned}$$

and therefore:

$$\|E(t)\|_{SO(3)} = \text{constant} = \|E(0)\|_{SO(3)}$$

Proof of Theorem 1:

Considering that $\widehat{\omega}_{gyr} = \widehat{\omega}$ by (21), the whole system (24) can be conveniently rewritten as:

$$\dot{R}^* = R^* (\widehat{\omega} + \sum_{i=1}^N k_i [\widehat{v}_i, \widehat{v}_i^*]) \tag{51}$$

where the (3) was used to rewrite the cross product in \mathbb{R}^3 in terms of the Lie commutator in $so(3)$.

Following [5], define the estimation error E as in (22) and consider its time derivative $\dot{E} = \dot{R}^T R^* + R^T \dot{R}^*$. Use now (51) to write the dynamics of estimation error as:

$$\begin{aligned}
E^T \dot{E} &= R^{*T} R \dot{R}^T R^* + R^{*T} R R^T \dot{R}^* \\
&= R^{*T} R \dot{R}^T R^* + R^{*T} \dot{R}^* \\
&= R^{*T} R \dot{R}^T R^* + \widehat{\omega} + \sum_{i=1}^N k_i [\widehat{v}_i, \widehat{v}_i^*] \\
&= R^{*T} R \dot{R}^T R R^T R^* + \widehat{\omega} + \sum_{i=1}^N k_i [\widehat{v}_i, \widehat{v}_i^*] \\
&= E^T \dot{R}^T R E + \widehat{\omega} + \sum_{i=1}^N k_i [\widehat{v}_i, \widehat{v}_i^*]
\end{aligned}$$

Note that $\frac{d}{dt} (R^T R) = \frac{d}{dt} (I) = 0$ implies that $\dot{R}^T R + R^T \dot{R} = 0$ and therefore:

$$E^T \dot{E} = -E^T \widehat{\omega} E + \widehat{\omega} + \sum_{i=1}^N k_i [\widehat{v}_i, \widehat{v}_i^*] \tag{52}$$

In order to prove stability, as in [5], the natural norm on $SO(3)$ defined in (6) is chosen as a positive-definite candidate Lyapunov function $W(E)$, i.e.:

$$W(E) \triangleq \frac{1}{2} \|E\|_{SO(3)} = \frac{1}{2} \langle \langle \log(E), \log(E) \rangle \rangle_{so(3)}^{1/2} \tag{53}$$

where $\log(E) = \widehat{\phi}_E \in so(3)$ is defined in (8) while $\langle \langle \cdot, \cdot \rangle \rangle_{so(3)}$ is the bi-invariant metric defined in (5).

The time derivative of $W(E)$ can be computed via (7) as:

$$\dot{W}(E) = \frac{1}{2} \frac{d}{dt} \|E\|_{SO(3)} = \langle \langle \log(E), E^T \dot{E} \rangle \rangle_{so(3)}$$

Substituting (52):

$$\dot{W}(E) = \langle \langle \log(E), -E^T \widehat{\omega} E + \widehat{\omega} \rangle \rangle_{so(3)} + \langle \langle \log(E), \sum_{i=1}^N k_i [\widehat{v}_i, \widehat{v}_i^*] \rangle \rangle_{so(3)} \tag{54}$$

As shown in Lemma 2, the first term in the right side of the last equation is always zero and therefore

$$\dot{W}(E) = \langle \langle \log(E), \sum_{i=1}^N k_i [\widehat{v}_i, \widehat{v}_i^*] \rangle \rangle_{so(3)} \tag{55}$$

Equation $v_i = R^T v_{0i}$ from (21) and equation $v_i^* = R^{*T} v_{0i}$ from (24) lead to

$$v_i = E v_i^*$$

therefore, recalling (3) and (5), $\dot{W}(E)$ can be written in terms of \mathbb{R}^3 vectors as:

$$\begin{aligned}
\dot{W}(E) &= \phi_E^T \left(\sum_{i=1}^N k_i ((E v_i^*) \times v_i^*) \right) \\
&= \sum_{i=1}^N k_i \phi_E^T ((E v_i^*) \times v_i^*)
\end{aligned}$$

In order to study the sign of $\dot{W}(E)$, it is convenient to express E as a function of ϕ_E via the Rodrigues' formula (9):

$$E = \exp(\widehat{\phi}_E) = I + \alpha_E \widehat{\phi}_E + \beta_E \widehat{\phi}_E^2 \tag{56}$$

$$\text{where } \begin{cases} \alpha_E = \frac{\sin \|\phi_E\|}{\|\phi_E\|} \\ \beta_E = \frac{1 - \cos \|\phi_E\|}{\|\phi_E\|^2} \end{cases} \tag{57}$$

and rewrite:

$$\dot{W}(E) = \sum_{i=1}^N k_i \phi_E^T ((v_i^* + \alpha_E \widehat{\phi}_E v_i^* + \beta_E \widehat{\phi}_E^2 v_i^*) \times v_i^*) \tag{58}$$

Consider the following identities for all $\phi, v \in \mathbb{R}^3$:

$$\begin{aligned}
v \times v &= 0 \\
(\widehat{\phi} v) \times v &= (\phi^T v) v - \|v\|^2 \phi \\
\phi^T ((\widehat{\phi}^2 v) \times v) &= 0
\end{aligned}$$

which allow writing:

$$\begin{aligned}
\dot{W}(E) &= \sum_{i=1}^N k_i \phi_E^T ((\alpha_E \widehat{\phi}_E v_i^*) \times v_i^*) \\
&= \sum_{i=1}^N k_i \alpha_E ((\phi_E^T v_i^*)^2 - \|v_i^*\|^2 \|\phi_E\|^2)
\end{aligned} \tag{59}$$

Recalling that, by the dot product in \mathbb{R}^3 , $\phi_E^T v_i^* = \|\phi_E\| \|v_i^*\| \cos \theta_i$ where θ_i is the angle between ϕ_E and v_i^* , a since, as in (56), $\alpha_E = \sin \|\phi_E\| / \|\phi_E\|$, we can write:

$$\dot{W}(E) = - \sum_{i=1}^N k_i \sin \|\phi_E\| \|\phi_E\| \|v_i^*\|^2 (1 - \cos^2 \theta_i) \tag{60}$$

moreover, since $v_i^* = R^{*T}v_{0i}$ and $R^* \in SO(3)$ then $\|v_i^*\| = \|v_{0i}\|$, and then

$$\dot{W}(E) = -\|\phi_E\| \sin \|\phi_E\| \sum_{i=1}^N k_i \|v_{0i}\|^2 (1 - \cos^2 \theta_i) \quad (61)$$

Consider the following inequality

$$\sum_{i=1}^N k_i \|v_{0i}\|^2 (1 - \cos^2 \theta_i) \geq \sum_{i=1}^2 k_i \|v_{0i}\|^2 (1 - \cos^2 \theta_i)$$

since $k_i > 0$, θ_i represents the alignment between ϕ_E and v_i and since v_1 and v_2 are assumed independent in (20), ϕ_E can never be aligned, at the same time, with both v_1 and v_2 . Therefore θ_1 and θ_2 can never be zero at the same time. This implies that $\exists \gamma > 0$ such that

$$\begin{aligned} \sum_{i=1}^N k_i \|v_{0i}\|^2 (1 - \cos^2 \theta_i) &\geq \\ &\geq \sum_{i=1}^2 k_i \|v_{0i}\|^2 (1 - \cos^2 \theta_i) \geq \gamma > 0 \end{aligned}$$

therefore, recalling from (53) that $W(E) = 1/2 \|\phi_E\|^2$, we can write

$$\dot{W}(E) \leq -\gamma \sqrt{2W(E)} \sin \sqrt{2W(E)} \quad (62)$$

or, simplifying the notation,

$$\dot{W} \leq -\gamma \sqrt{2W} \sin \sqrt{2W} \quad (63)$$

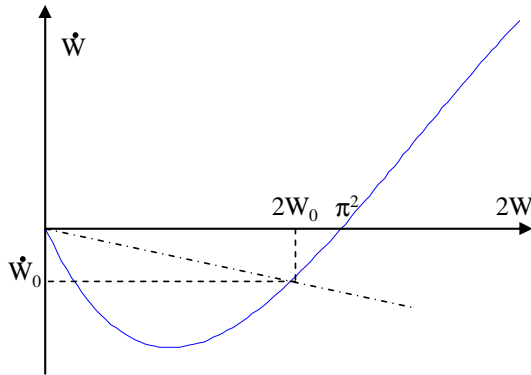


Fig. 8. Plot of the function $\dot{W} = -\gamma \sqrt{2W} \sin \sqrt{2W}$ vs. $2W$.

For any initial configuration $E(0)$ such that $\text{trace}(E(0)) \neq -1$, the logarithmic map (8) guarantees that $\|\phi_E\| < \pi$, i.e. the following holds for $W_0 \triangleq 2W(E(0))$:

$$0 \leq 2W_0 < \pi^2$$

In such an interval, as shown in Fig. 8, a linear upper bound can always be found such that:

$$\dot{W} \leq -\lambda \sqrt{2W} \sin \sqrt{2W} \leq \frac{\dot{W}_0}{W_0} W = -\eta W$$

where $\eta > 0$ since $\dot{W}_0 = \dot{W}(E(0)) < 0$. This finally proves convergence since the linear upper bound can easily be integrated, leading to:

$$0 < W(t) \leq W_0 e^{-\eta t} \Rightarrow \lim_{t \rightarrow \infty} W(t) = 0$$

Since $W(t) = W(E(t))$ measures the distance between $E = R^T(t)R^*(t)$ and $I \in SO(3)$, then:

$$\lim_{t \rightarrow \infty} R^T(t)R^*(t) = I$$

■

REFERENCES

- [1] V. I. Arnold, “*Mathematical Methods of Classical Mechanics*”, 2nd ed., Springer-Verlag, New York, 1989.
- [2] R. G. Brown and P. Y. C. Hwang, “*Introduction to random signals and applied Kalman filtering*”, New York: J. Wiley, 1992.
- [3] F. Bullo and A. D. Lewis, “*Geometric Control of Mechanical Systems*”, Springer, 2005.
- [4] F. Bullo and R. M. Murray, “*Tracking for Fully Actuated Mechanical Systems: a Geometric Framework*”, *Automatica*, Vol. 35, No. 1, pp. 17-34 Jan. 1999.
- [5] F. Bullo and R. F. Murray “*Proportional derivative (PD) Control on the Euclidean Group*”, Technical report, California Institute of Technology, Anaheim, CA USA, 1995.
- [6] D. Campolo, F. Keller, E. Guglielmelli, “*Inertial/Magnetic Sensors Based Orientation Tracking on the Group of Rigid Body Rotations with Application to Wearable Devices*”, *IEEE/RSJ Int. Conf. on Intelligent Robots and Systems (IROS)*, Beijing, P.R. China, October 9-14, 2006.
- [7] J. Chahl, “*Bioinspired Engineering of Exploration Systems: A Horizon Sensor/Attitude Reference System Based on the Dragonfly Ocelli for Mars Exploration Applications*”, *Journal of Robotic Systems*, Vol. 20, No. 1, pp. 35-42 2003.
- [8] Commonwealth Scientific and Industrial Research Organisation (CSIRO), URL: <http://www.csiro.au/>.
- [9] F. Daum, “*Nonlinear Filters: Beyond the Kalman Filter*”, *IEEE A&E Systems Magazine*, Vol.20, No. 8, August 2005.
- [10] X. Deng and L. Schenato and W.C. Wu and S.S. Sastry, “*Flapping Flight for Biomimetic Robotic Insects. Part I: System modeling*”, *IEEE Transactions on Robotics*, Vol. 22, No. 4, pp. 789- 803, 2006.
- [11] X. Deng and L. Schenato and S.S. Sastry, “*Flapping Flight for Biomimetic robotic Insects. Part II: Flight Control Design*”, *IEEE Transactions on Robotics*, Vol. 22, No. 4, pp. 789- 803, 2006.
- [12] M.H. Dickinson, “*Linear and nonlinear encoding properties of an identified mechanoreceptor on the fly wing measured with mechanical noise stimuli*”, *The Journal of Experimental Biology*, Vol. 151, pp. 219-244, 1990.
- [13] M. Epstein, S. Waydo, S.B. Fuller, W. Dickson, A. Straw, M.H. Dickinson, and R.M. Murray, “*Biologically Inspired Feedback Design for Drosophila Flight*”, to appear in *Proc. of IEEE American Control Conference*, 2007.
- [14] R.S. Fearing, K.H. Chiang, M.H. Dickinson, D.L. Pick, M. Sitti, J. Yan, “*Wing Transmission for a Micromechanical Flying Insect*”, in *Proc. of IEEE Intl. Conf. on Robotics and Automation*, pp. 1509-1516, 2000.
- [15] T. Frankel, “*The Geometry of Physics: an Introduction*”, Cambridge University Press, Cambridge, UK, 1997.
- [16] J. Grasmeyer and M.T. Keennon, “*Development of the black widow micro air vehicle*”, in *39th AIAA Aerospace Sciences Meeting and Exhibit*, 2001.
- [17] R. Hengstenberg, “*Mechanosensory control of compensatory head roll during flight in the blowfly Calliphora erythrocephala*”, *Journal of Comparative Physiology A-Sensory Neural & Behavioral Physiology*, Vol. 163, pp. 151-165, 1988.
- [18] J.P. How, E. King, and Y. Kuwata, “*Flight Demonstrations of Cooperative Control for UAV Teams*”, in *AIAA 3rd Unmanned Unlimited Technical Conference*, pp. 1509-1516, 2004.
- [19] H.J. Kim and D.H. Shim and S.Sastry, “*A Flight Control System for Aerial Robots: Algorithms and Experiments*”, *Control Engineering Practice*, Vol. 11, No. 12, pp. 1389-1400, 2003.
- [20] I. Kroo and P. Kunz, “*Development of the Mesicopter: A Miniature Autonomous Rotorcraft*”, in *American Helicopter Society (AHS) Vertical Lift Aircraft Design Conference*, 2000.
- [21] D. E. Koditschek, “*The application of total energy as a Lyapunov function for mechanical control systems*”, in J. E. Marsden, P. S. Krishnaprasad & J. C. Simo (eds), *Dynamics and Control of Multibody Systems*, Vol. 97, AMS, pp. 131-157, 1989.
- [22] D. Lambros, H. Kobayashi, R. Pfeifer, M. Maris, T. Labhart, R. Wehner, “*Adaptive Behavior An Autonomous Agent Navigating with a Polarized Light Compass*”, *Adaptive Behavior*, Vol. 6, No. 1, pp. 131-161, 1997.

- [23] D. H. S. Maithripala, J. M. Berg, and W. P. Dayawansa, “*Almost-Global Tracking of Simple Mechanical Systems on a General Class of Lie Groups*”, IEEE Trans. on Automatic Control, Vol. 51, No. 1, Jan. 2006.
- [24] D. H. S. Maithripala, J. M. Berg and W. P. Dayawansa, “*An Intrinsic Observer for a Class of Simple Mechanical Systems on a Lie Group*”, SIAM Journ. Control Optim., Vol. 44, No. 5, pp. 1691-1711, Nov. 2005.
- [25] R.C. Michelson and M.A. Naqvi, “*Beyond Biologically Inspired Insect Flight*”, in von Karman Institute for Fluid Dynamics RTO/AVT Lecture Series on “Low Reynolds Number Aerodynamics on Aircraft Including Applications in Emergening UAV Technology”, pp. 1-19, Brussels, Belgium, 2003.
- [26] R. M. Murray, Z. Li, and S. S. Sastry, “*A Mathematical Introduction to Robotic Manipulation*”, CRC, Boca Raton, FL, 1994.
- [27] G. Nalbach, “*The halteres of the blowfly Calliphora: I. Kinematics and dynamics*”, Journal of Comparative Physiology A, Vol. 173, pp. 293-300, 1993.
- [28] W. Reichardt and M. Egelhaaf, “*Properties of individual movement detectors as derived from behavioural experiments on the visual system of the fly*”, in Biological Cybernetics, Vol. 58, No. 5, pp. 287-294, 1988.
- [29] S.P. Sane and M.H. Dickinson, “*The control of flight force by a flapping wing: Lift and drag production*”, The Journal of Experimental Biology, Vol. 204, pp. 2607-2626, 2001.
- [30] S.P. Sane, “*The aerodynamics of insect flight*”, The Journal of Experimental Biology, Vol. 206, pp. 4191-4208, 2003.
- [31] S. S. Sastry, “*Nonlinear Systems: Analysis, Stability and Control*”, Springer, New York, 1999.
- [32] L. Schenato, W. C. Wu and S. S. Sastry, “*Attitude Control for a Micromechanical Flying Insect via Sensor Output Feedback*”, IEEE Trans. on Robotics and Automation, Vol.20, No. 1, pp. 93-106, Feb. 2004.
- [33] H. Schuppe and R. Hengstenberg, “*Optical properties of the ocelli of Calliphora erythrocephala and their role in the dorsal light response*”, Journal of Comparative Biology A, Vol. 173, pp. 143-149,1993.
- [34] G.K. Taylor, “*Mechanics and aerodynamics of insect flight control*”, Biological Review, Vol.76, No. 4, pp. 449-471, 2001.
- [35] Victoria Museum, URL: <http://www.museum.vic.gov.au/>.
- [36] E. Wajnberga and G. Cernicchiaroa and D. Acosta-Avalosb and L. J. El-Jaicka and D. M. S. Esquivel, “*Induced remanent magnetization of social insects*”, Journal of Magnetism and Magnetic Materials, Vol. 226-230, pp. 2040-2041, 2001.
- [37] J. Wessnitzer and B. Webb, “*Multimodal sensory integration in insects: towards insect brain control architectures*”, Bioinspiration & Biomimetics, Vol. 1, pp. 63-75, 2006.
- [38] W. C. Wu, R. J. Wood and R. F. Fearing, “*Halteres for the Micromechanical Flying Insect*”, in Proc. of IEEE Intl. Conf. on Robotics and Automation, pp. 60-65, 2002.
- [39] W. C. Wu, L. Schenato, R. J. Wood and R. F. Fearing, “*Biomimetic Sensor Suite for Flight Control of MFI: Design and Experimental Results*”, in Proc. of IEEE Intl. Conf. on Robotics and Automation, pp. 1146-1151, 2003.